Proceedings of the Combustion Institute SAND2020-1231C

Direct numerical simulations of turbulent stratified premixed jet combustion under MILD and conventional conditions

--Manuscript Draft--

Manuscript Number:	PROCI-D-19-00676
Article Type:	12. Gas Turbine/Rocket Combustion
Keywords:	MILD combustion; Stratified premixed; Auto-ignition; Direct numerical simulation
Corresponding Author:	Haiou Wang Zhejiang University Hangzhou, CHINA
First Author:	Haiou Wang
Order of Authors:	Haiou Wang
	Kun Luo
	Evatt R. Hawkes
	Jacqueline H. Chen
	Jianren Fan
Abstract:	Turbulent stratified premixed jet flames under moderate or intense low-oxygen dilution (MILD) and conventional conditions were studied using three-dimensional direct numerical simulations (DNS) in this work. The thermo-chemical conditions of the reactants in the DNS are determined by mixing a cold jet of C2H4/air and a hot vitiated flow. Two flames with different levels of mixing were investigated. One flame is located in the MILD combustion regime, denoted as case A, and the other one is in the conventional combustion regime, denoted as case B. The species budget and chemical explosive mode analysis (CEMA) were employed to determine the local combustion mode. Both flames were found to be stabilized by auto-ignition. Ignition starts in the leaner side, and then the reaction zone shifts to the richer side until all reactants are consumed. Case A is dominated by auto-ignition at different positions while flame propagation plays an important role in the downstream region of case B. Consistent results were obtained for both the DNS and one-dimensional unsteady reference laminar flames. The distributions of heat release rate and intermediate species are more homogeneous in case A than case B while their magnitude is lower. The flame structure is considerably influenced by shear-dominant turbulence, and local flame thickening is observed for the conventional flame due to the effects of small-scale turbulence. The modeling of MILD combustion was also investigated a priori and it was found that simple tabulation models based on one-dimensional unsteady laminar flames and homogeneous reactor perform reasonably well for the MILD flame, while the model performance deteriorates for the conventional flame.

Direct numerical simulations of turbulent stratified premixed jet combustion under MILD and conventional conditions

Haiou Wang[a,*], Kun Luo[a], Evatt R. Hawkes[b,c], Jacqueline H. Chen[d], Jianren Fan[a]

[a] *State Key Laboratory of Clean Energy Utilization, Zhejiang University, Hangzhou 310027, PR China*
[b] *School of Manufacturing and Mechanical Engineering, University of New South Wales, Sydney, NSW, 2052, Australia*
[c] *School of Photovoltaics and Renewable Energy Engineering, University of New South Wales, Sydney, NSW, 2052, Australia*
[d] *Sandia National Laboratories, Livermore, CA 94550, USA*

Abstract

Turbulent stratified premixed jet flames under moderate or intense low-oxygen dilution (MILD) and conventional conditions were studied using three-dimensional direct numerical simulations (DNS) in this work. The thermo-chemical conditions of the reactants in the DNS are determined by mixing a cold jet of C_2H_4/air and a hot vitiated flow. Two flames with different levels of mixing were investigated. One flame is located in the MILD combustion regime, denoted as case A, and the other one is in the conventional combustion regime, denoted as case B. The species budget and chemical explosive mode analysis (CEMA) were employed to determine the local combustion mode. Both flames were found to be stabilized by auto-ignition. Ignition starts in the leaner side, and then the reaction zone shifts to the richer side

*Corresponding author: Haiou Wang
Email address: wanghaiou@zju.edu.cn (Haiou Wang)

until all reactants are consumed. Case A is dominated by auto-ignition at different positions while flame propagation plays an important role in the downstream region of case B. Consistent results were obtained for both the DNS and one-dimensional unsteady reference laminar flames. The distributions of heat release rate and intermediate species are more homogeneous in case A than case B while their magnitude is lower. The flame structure is considerably influenced by shear-dominant turbulence, and local flame thickening is observed for the conventional flame due to the effects of small-scale turbulence. The modeling of MILD combustion was also investigated *a priori* and it was found that simple tabulation models based on one-dimensional unsteady laminar flames and homogeneous reactor perform reasonably well for the MILD flame, while the model performance deteriorates for the conventional flame.
Keywords:
MILD combustion, Stratified premixed, Auto-ignition, Direct numerical simulation

1. Introduction

Combustion technologies exist to reduce pollutant emissions and improve combustion efficiency, among which moderate or intense low-oxygen dilution (MILD) combustion [1, 2] is a promising solution for lowering NO_x formation and achieving better efficiency. Compared to conventional combustion, the reactant temperature, T_{in}, in MILD combustion is elevated and the temperature increase is reduced [2]. In particular, for MILD combustion, T_{in} is higher than the auto-ignition temperature of the reactants, T_{ig}, so that

auto-ignition can occur while the maximum temperature rise, ΔT, is lower than T_{ig}. In practice, this can be accomplished by preheating and dilution with inert gas [3] or exhaust gas recirculation [4]. Currently, there are a few examples of MILD combustion in furnaces and gas turbines [5]. However, existing understanding of these applications is insufficient. In order to further improve the performance of practical combustors, it is imperative to gain more fundamental understandings of the physics involved in MILD combustion.

One significant feature of MILD combustion is the reduced luminous emission compared to conventional combustion. This indicates that there are notable differences in the thermochemical structure between the two combustion types. Several laboratory-scale experiments of MILD combustion with laser diagnostics have been performed [4, 6, 7], providing information of the flame structure in various configurations. The distributions of OH and temperature in MILD combustion were measured in [4]. It was shown that the OH intensity was much lower and the temperature was more homogeneous in the MILD case. Temperature and major species concentrations in a jet-in-hot-coflow (JHC) configuration were presented in [6]. By decreasing the oxygen level in the hot coflow, the luminosity and the levels of NO were reduced. In the above studies, fuel and oxidizer were introduced separately from the inlet, and the flames were lifted in hot environment.

MILD combustion in premixed conditions has received less attention in the literature. Duwig *et al.* [8] investigated premixed MILD combustion with different equivalence ratios. The reaction zones were distributed due to the interplay between flames and shear turbulence, and the flame base

was also observed to be lifted. Wagner *et al.* [9] conducted experiments of a premixed reacting jet in a vitiated crossflow, which is relevant to MILD combustion [2, 10]. It was suggested auto-ignition was dominant for the windward flame stabilization while flame propagation is dominant for the leeward flame stabilization, and this was later confirmed by the large eddy simulation (LES) results of Schulz *et al.* [10]. In all these configurations, the jet equivalence ratio is different than that in the coflow. Consequently, the equivalence ratio in the reaction zone varies between the equivalence ratio of the jet and coflow. Therefore, 'stratified premixed' is a more accurate description than 'premixed' to describe these flames [11, 12].

Due to its importance, MILD combustion has also been widely studied with LES and Reynolds-averaged Navier-Stokes (RANS) [10, 13–16]. Direct numerical simulation (DNS) represents a very useful tool for understanding the fundamentals of turbulent combustion. It was recently employed for MILD combustion. Particularly, van Oijen [17] performed two-dimensional (2D) DNS of non-premixed jet flames following the JHC experiments of Dally *et al.* [6]. Minamoto *et al.* [18] performed 3D DNS of premixed MILD combustion in isotropic turbulence. This work was further extended to partially premixed combustion by Doan *et al.* [19]. Despite these studies, to our best knowledge, no DNS of stratified premixed flames with complex shear turbulence under MILD conditions has been reported.

In the above context, the objectives of the present study are as follows. First, 3D DNS of stratified premixed slot-jet flames under MILD and conventional conditions is performed. The DNS results are compared to those of the corresponding 1D laminar flames to understand the effects of complex

shear turbulence on combustion. Second, the ignition process and flame stabilization mechanism of MILD and conventional flames are explored. The roles of auto-ignition and flame propagation are identified. Finally, models for predicting turbulent stratified premixed MILD combustion are examined, and the performance of the models is evaluated *a priori*.

2. Simulation details

A slot-jet configuration with a coflow and a central jet is employed in the present work. The coflow of the DNS is the same as in the experiment [9], generated from lean C_3H_8/air combustion with an equivalence ratio of 0.87, and the coflow temperature is 1500 K. The thermochemical conditions of the central jet are determined by adiabatically mixing the coflow and a cold jet (C_2H_4/air mixture with a temperature of 300 K and an equivalence ratio of 1.2). Two cases with different levels of mixing, denoted as case A and case B, are considered. The resultant equivalence ratio of the central jet, ϕ_j, is 0.97 and 1.07 for case A and case B, respectively. The temperature of the central jet, T_j, is 1181 K and 823 K for case A and case B, respectively. The composition of the coflow and central jet is provided in the supplementary material.

The thermochemical conditions of the two cases are determined so that they are located in different regimes of the combustion type diagram [2] as presented in Fig. 1. The ignition temperature T_{ig} was obtained from homogeneous reactor simulations at constant pressure with Cantera [20]. The central jet mixture of case A is auto-ignitive with an ignition delay time τ_{ig} of 1.6 ms, while that of case B is two orders of magnitude larger based on

homogeneous reactor simulations. As can be seen in Fig. 1, case A with a higher level of dilution is in the MILD combustion regime while case B with a lower level of dilution is in the conventional combustion regime. It is noted that the combustion regime results should only be interpreted qualitatively.

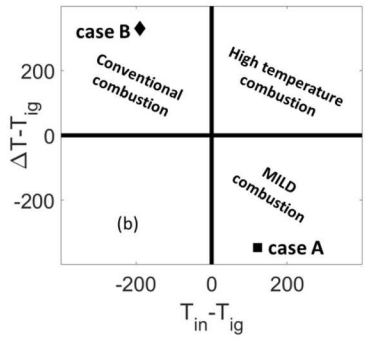

Figure 1: Different combustion regimes for the present study.

The jet velocity U_j is 300 m/s and 163 m/s for case A and case B, respectively, so that the jet Reynolds number is the same for both cases. The coflow velocity U_c is 7.6 m/s. The mean velocity profile at the inlet is given as: $U = U_j + \frac{U_c - U_j}{2}[1 + tanh(\frac{y-H/2}{\delta})tanh(\frac{y+H/2}{\delta})]$, where the jet width H is 1.5 mm, and the shear layer thickness δ is specified as $0.1H$. The jet Reynolds number based on U_j and H is $Re_j = 2880$. The profile of a scalar ψ (temperature or species mass fractions) at the inlet is similar to that in Wang *et al.* [21] with a smooth transition between the jet and the coflow. A turbulence field is obtained by generating an auxiliary homogeneous isotropic turbulence. The turbulent velocity u' is 10% of U_j for both cases and the integral length scale l_t is is the same as H, *i.e.* 1.5 mm. The isotropic turbulence field is then filtered outside of the jet and added to the mean inlet velocity using Taylor's hypothesis. The other simulation parameters are listed in Ta-

Table 1: Simulation parameters for the DNS

case	s_L (m/s)	δ_L (mm)	Re_T $(\frac{u'l_t}{s_L\delta_L})$	Da $(\frac{s_Ll_t}{u'\delta_L})$
A	2.0	0.615	37	0.16
B	1.7	0.374	38	0.42

ble 1, where the reference laminar premixed flame velocity s_L and thickness δ_L for case A are determined in a similar way as Ref. [22] for auto-ignitive mixtures.

The computational domain is $L_x \times L_y \times L_z = 40H \times 40H \times 10H$ in the streamwise x, traverse y, and spanwise z directions, respectively, for case A. To capture the entire flame, L_x is increased to $60H$ for case B. The grid spacing is chosen to resolve the flame and turbulence structures. Particularly, a uniform grid with $\Delta x = 50$ μm and $\Delta z = 37.5$ μm is used in the streamwise and spanwise directions, respectively. A stretched grid is used in y direction with $\Delta y = 37.5$ μm in the region between y/H = -5 and 5, and gradually stretched outside of this region. There is at least 0.5 grid point across the Kolmogorov scale, η, throughout the computational domain, satisfying the criterion for resolving turbulence scales. The resultant number of grids is $N_x \times N_y \times N_z = 1200 \times 800 \times 400$ for case A and $N_x \times N_y \times N_z = 1800 \times 800 \times 400$ for case B. The boundary conditions are periodic in the spanwise direction and non-reflecting in other directions [23].

The DNS code S3D [24] was employed in the present work. It solves the compressible governing equations of mass continuity, momentum, total energy and mass fractions of chemical species including chemical reactions using high-order finite difference methods. Interested readers are referred to

Ref. [24] for numerical details. A reduced mechanism for C_2H_4 combustion was used [25]. This mechanism has been validated for various problems including auto-ignition and premixed flame propagation. The simulations were advanced for $3\tau_j$ after reaching a statistically steady state, where τ_j is the flow-through time estimated as $\tau_j = L_x/U_j$.

3. Chemical explosive mode analysis

One objective of the present work is to determine the role of auto-ignition and flame propagation. The chemical explosive mode analysis (CEMA) represents a promising tool for this purpose and has been employed for complex turbulent flames previously [10, 26, 27]. A detailed description of CEMA was provided by Refs. [26, 27], and it is briefly introduced here.

The transport equation for chemical source term $\boldsymbol{\omega}(\mathbf{y})$ can be written as:

$$\frac{D\boldsymbol{\omega}(\mathbf{y})}{Dt} = \mathbf{J}_{\boldsymbol{\omega}} \frac{D\mathbf{y}}{Dt} = \mathbf{J}_{\boldsymbol{\omega}}(\boldsymbol{\omega} + \mathbf{s}) \tag{1}$$

where $\mathbf{J}_{\boldsymbol{\omega}}$ is the chemical Jacobian ($\mathbf{J}_{\boldsymbol{\omega}} = D\boldsymbol{\omega}/D\mathbf{y}$) and $\mathbf{s}$ is the diffusion term. The eigenvalue of $\mathbf{J}_{\boldsymbol{\omega}}$ associated with the most explosive mode, *i.e.* the eigenvalue with the largest positive real part, is denoted as λ_e.

We follow the work of Xu *et al.* [27] and project the chemical and diffusion terms onto the most explosive eigenvector. The projected chemical and diffusion source terms are denoted as $\phi_{\boldsymbol{\omega}}$ and $\phi_{\mathbf{s}}$, respectively. Finally, a local combustion mode indicator, α, can be defined as $\alpha = \phi_{\mathbf{s}}/\phi_{\boldsymbol{\omega}}$. Based on the definition, α measures the relative importance of diffusion compared to reaction so that different local combustion modes can be identified. Particularly, $\alpha > 1$ indicates a diffusion-assisted ignition mode, $|\alpha| \leq 1$ indicates

a local auto-ignition mode, and $\alpha < -1$ indicates a local extinction mode. The CEMA results for different cases will be discussed in the next section.

4. Results and discussion

4.1. 1D laminar flames

Before showing the DNS results, 1D unsteady reference laminar flames are presented. Two laminar cases, namely case LA and case LB, were considered. They correspond to the two DNS cases, *i.e.* case A and case B, respectively. The initial profiles of temperature and species mass fractions in 1D cases are the same as in the DNS cases, and the initial velocity is zero.

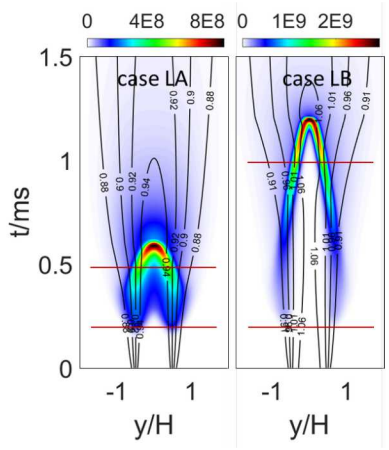

Figure 2: Evolution of heat release rate (J/m^3s) in 1D laminar flames. The black lines show the equivalence ratio iso-lines. The red lines outline $t = 0.2$ ms and 0.5 ms for case LA and $t = 0.2$ ms and 1.0 ms for case LB.

The evolution of heat release rate for 1D cases is presented in Fig. 2. It is seen that for both cases the ignition occurs at about $t = 0.2$ ms. The ignition starts in the leaner side close to the coflow, due to a higher local

temperature. Later, the reaction zone shifts to the richer side until all the reactants are consumed.

Most of the reactions complete before $t = 0.6$ ms for case LA and $t = 1.2$ ms for case LB. Note that τ_{ig} for the reactants of case LA is about 1.6 ms while that of case LB is over 200 ms. There are two explanations for the discrepancies between the reaction time and τ_{ig}. First, the reactants are surrounded by a hot vitiated coflow. The mixing between the reactants and coflow facilitates the ignition process and the thermal runaway after ignition. Second, a flame could develop after ignition so that the flame front propagates into the reactants. The former is likely to play a role in both cases, at least during the ignition process, while the latter seems to occur in case LB, responsible for the large difference between the reaction time and τ_{ig} for case LB.

The relative importance of auto-ignition and propagation is revealed by examining the contribution of reaction and diffusion in the species transport equations. The budget analysis has been used for identifying the role of auto-ignition [28]. Fig. 3 shows the profiles of the species budget of CO and heat release rate at different time outlined in Fig. 2 for case LA and case LB. The species CO is selected as it represents a key species in the reaction zone. At the ignition time of $t = 0.2$ ms, the reaction term is much larger than the diffusion term for both cases. This indicates both flames are stabilized by auto-ignition. At $t = 0.5$ ms for case LA, the reaction term is still dominant over the diffusion term. The scenario is different at $t = 1.0$ ms for case LB, which shows that the diffusion and reaction terms are of the same order of magnitude. The balance between reaction and diffusion is an indication of

flame propagation [28].

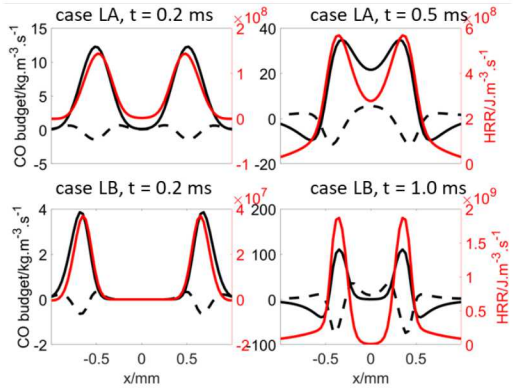

Figure 3: The profiles of CO reaction term (black solid line), CO diffusion term (black dashed line), and heat release rate (red solid line) in the laminar flames.

The budget analysis is complemented by CEMA, which has been widely used in previous studies to distinguish the local combustion modes, *i.e.* auto-ignition versus flame propagation [10, 26]. Fig. 4 shows the evolution of the local combustion mode indicator, α, on which iso-lines of progress variable (c) are superimposed. Regions with $\lambda_e < 0$ and slow reactions are truncated. The progress variable c is defined based on the mass fraction of H_2O and it increases monotonically from zero in the reactants to unity in the products. It is shown that the auto-ignition mode is dominant in the reactant side for $c > 0.1$ for case LA, while diffusion-assisted ignition is dominant for case LB, characteristics of a propagating flame. The CEMA results are therefore consistent with the budget analysis shown in Fig. 3.

4.2. 3D turbulent stratified jet flames

Figure 5 shows the instantaneous distributions of heat release rate, equivalence ratio, and species mass fractions of CO, CH_2O and OH for case A and

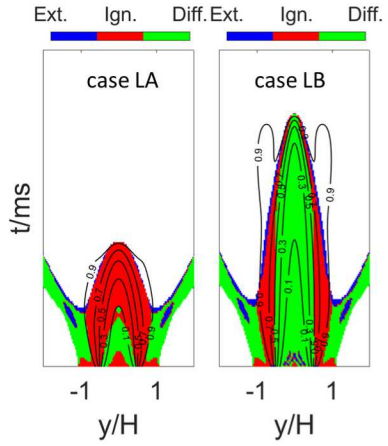

Figure 4: Evolution of the local combustion mode indicator α in the 1D laminar flames. The black lines delineate the progress variable iso-surface.

case B. As can be seen, both flames are lifted and the lift-off height is about $8H$ for case A and $2H$ for case B. Several other observations can be made.

First, the distribution of heat release rate is nearly uniform in case A while thin reaction fronts exist in case B. Uniform distributions of temperature and intermediate species in MILD combustion were revealed in experiments [4, 5, 7]. Thin flame structures are observed in case B under conventional conditions. Local flame thickening due to flame-turbulence interactions is also seen, which has been investigated in Wang *et al.* [21].

Second, both cases undergo mixture stratification with a higher equivalence ratio in the jet and lower equivalence ratio in the coflow, *i.e.* the flames are stratified premixed. The equivalence ratio field is significantly affected by the shear-dominant turbulence.

Third, the distributions of intermediates such as CO, CH_2O and OH are more homogeneous in case A than in case B. Moreover, the magnitude of

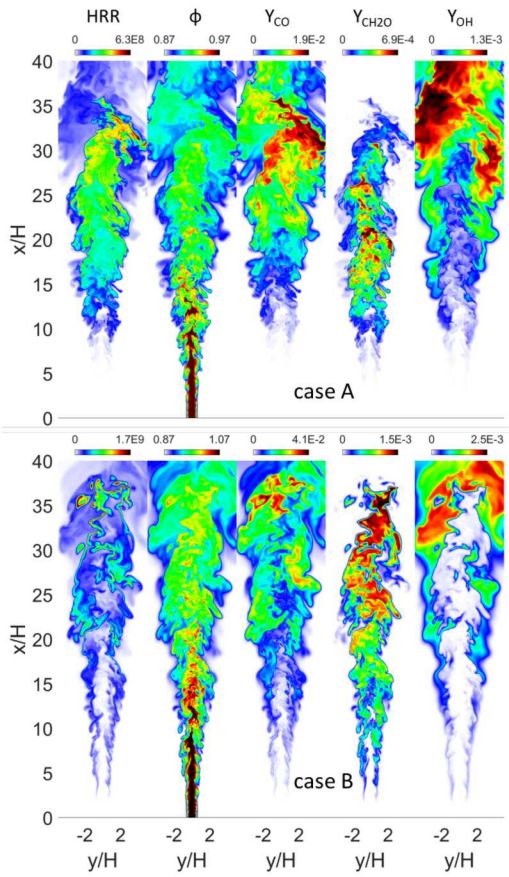

Figure 5: Distributions of heat release rate ($J/m^3 \cdot s$), equivalence ratio, and species mass fractions of CO, CH_2O and OH in a typical $x - y$ plane.

their concentrations in case A is about half of that in case B. These results are consistent with previous studies of MILD combustion with lower concentrations of intermediates [4–7], and possibly weaker luminosity.

Finally, it is of interest to compare the turbulent flame structure with the corresponding laminar flames in Sec. 4.1. Compared to the laminar flames, the reaction zone is more homogeneous for case A while it is disturbed for

case B due to turbulence.

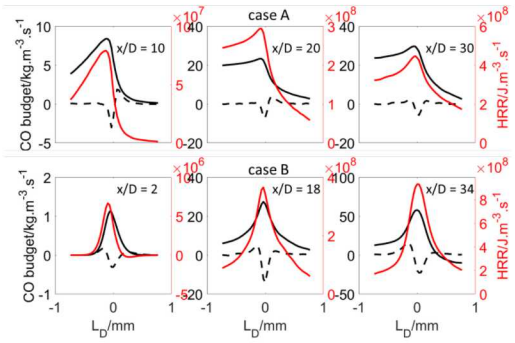

Figure 6: The profiles of CO reaction term (black solid line), CO diffusion term (black dashed line), and heat release rate (red solid line) conditioned on the distance function in the DNS.

The species budget of the turbulent cases is examined to identify the combustion mode as done in the laminar flames. Several previous DNS studies of turbulent combustion showed species budgets locally along the flame normal direction [18, 29]. It is, however, important to develop a method for revealing the general feature of species budget in highly turbulent flames, where a normal vector definition may be ambiguous in highly curved regions. As in Wang *et al.* [30], we calculate the species budget conditionally averaged on distance function. The distance function, L_D, is defined such that at each point in the computational domain it signifies the shortest normal distance to the flame front, computed by solving the Eikonal equation: $|\nabla L_D| = 1$. The value of L_D is set to zero at $c = 0.84$ (corresponding to the maximum heat release rate location) in both cases, and is negative in the reactants and positive in the products.

Figure 6 shows the profiles of CO budget and heat release rate conditioned

on L_D at different downstream locations for case A and case B. As can be seen, the reaction term is consistently larger than the diffusion term in case A under MILD combustion conditions. This implies that case A is dominated by auto-ignition at different axial locations. A different picture emerges for case B. Reaction is much larger than diffusion at $x/H = 2$, indicating the flame is stabilized due to auto-ignition; at $x/H = 18$ and 34, reaction and diffusion terms are balanced indicating the existence of a propagating flame.

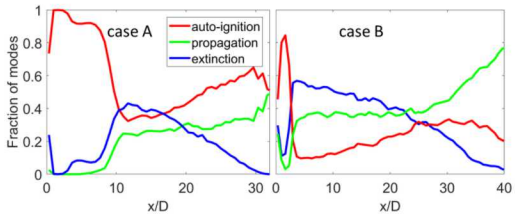

Figure 7: Axial evolution of the fraction of different combustion modes based on CEMA. The results are conditioned on $c = 0.7$.

In addition to the budget analysis, CEMA is also employed to distinguish the different combustion modes. Again, the local combustion mode indicator, α, is used as described in Sec.3. In turbulent flames, the distribution of α is quite complex, so only its statistics are presented. Fig. 7 shows the fraction of different combustion modes determined by α. The results are conditioned on the preheat zone with $c = 0.7$, similar to Ref. [27]. The results are similar in other regions of the preheat zone. It is confirmed that auto-ignition is dominant in case A as expected for MILD combustion, while flame propagation is playing a more important role for case B where conventional combustion is dominant in the downstream region.

4.3. Modeling implications

There exist RANS and LES modeling of MILD combustion [13–16], most of which focused on *a posteriori* studies of combustion models. DNS offers a unique way to directly test the underlying assumptions in combustion models and it was used to validate the tabulation models of MILD combustion in isotropic turbulence [18]. It was highlighted that the choice of model reactor is crucial [18]. In the present study, *a priori* studies of two tabulation models, based on 1D unsteady laminar flame simulations (see Sec. 4.1) and homogeneous reactor simulations (see Sec. 2), are performed for the current DNS flames in complex sheared turbulence.

Figure 8 shows the heat release rate conditioned on the progress variable, $\langle \dot{\omega}_T | c \rangle$, for different equivalence ratios of the stratified premixed flames. The results from the DNS and tabulation models are presented. The performance of the models differs in the two flames. In particular, in case A with MILD combustion both the models provide reasonable predictions, while in case B with conventional combustion their performance deteriorates. Based on the analysis in previous sections, auto-ignition is dominant in case A such that simple tabulation models such as the homogeneous reactor model perform well. This is consistent with the study of [18]. In contrast, in case B molecular diffusion and turbulent mixing strongly influences the inner layer of the flame, and hence more sophisticated models are needed for its accurate modeling. The effects of diffusion and strain rate on the model results will be explored in future work.

The model performance is further assessed by plotting in Fig. 9 the PDF of the progress variable weighted by heat release rate, *i.e.* $P_{\dot{\omega}_T}(c)$, which is

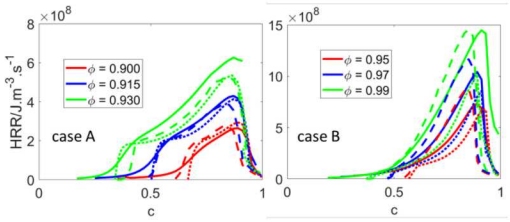

Figure 8: Heat release rate conditioned on the progress variable for different equivalence ratios. The results are from DNS (solid lines), 1D unsteady laminar flame simulations (dashed lines), and 0D reactor simulations (dotted lines).

calculated as $P_{\dot{\omega}_T}(c) = \langle \dot{\omega}_T | c \rangle \cdot P(c)/\overline{\dot{\omega}}_T$. Here, $\langle \dot{\omega}_T | c \rangle$ is taken from Fig. 8 and $P(c)$ is from the DNS. It is encouraging to see that the homogeneous reactor model provides almost the same weighted PDF as the DNS for case A, while a slight difference is observed for the 1D unsteady laminar flame model for $\phi = 0.9$ and $\phi = 0.93$. Larger discrepancies are observed between the DNS and models for case B. These are consistent with the results of Fig. 8.

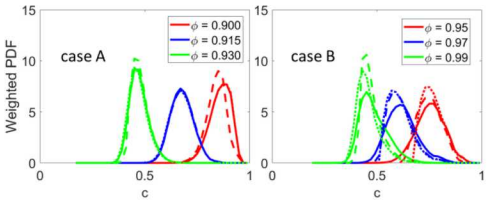

Figure 9: PDF of the progress variable weighted by heat release rate for different equivalence ratios. The results are from DNS (solid lines), 1D unsteady laminar flame simulations (dashed lines), and 0D reactor simulations (dotted lines).

5. Conclusions

In the present work, DNS was performed in a turbulent slot-jet configuration to understand the flame structure and modeling implications of turbulent stratified premixed flames under MILD and conventional conditions. The MILD combustion case is denoted as case A and the conventional combustion case as case B. 1D unsteady laminar flames were also simulated to provide a reference for the turbulent cases. Species budget analysis and CEMA were employed to identify the combustion modes. The following conclusions can be drawn from this work. *First*, both the DNS and 1D simulation results show that the flames are stabilized by auto-ignition. For case A, auto-ignition occurs consistently throughout the flame, while for case B, flame propagation plays an important role in the downstream region. *Second*, the complex shear turbulence has significant effects on the flame structures. Homogeneous distributions of species are observed in case A while the reaction zone is considerably disturbed in case B due to turbulence. *Finally*, simple tabulation models such as 1D laminar flame model and the homogeneous reactor model perform reasonably well for MILD combustion, while larger discrepancies between the DNS and models are observed for conventional combustion based on the *a priori* results.

Acknowledgments

This work was supported by Natural Science Foundation of China (Grant No.: 51976185, 91841302).

References

[1] M. Katsuki, T. Hasegawa. The science and technology of combustion in highly preheated air. Proc. Combust. Inst. 27 (1998) 3135–3146.

[2] A. Cavaliere, M. D. Joannon. Mild Combustion. Prog. Energy Combust. Sci. 30 (2004) 329–366.

[3] M. D. Joannon, G. Sorrentino, A. Cavaliere. MILD combustion in diffusion-controlled regimes of Hot Diluted Fuel. Combust. Flame 159 (2012) 1832–1839.

[4] T. Plessing, N. Peters, J. G. Wünning. Laseropticcal investigation of highly preheated combustion with strong exhaust gas recirculation. Proc. Combust. Inst. 27 (1998) 3197–3204.

[5] P. Li, B. B. Dally, J. Mi, F. Wang. MILD oxy-combustion of gaseous fuels in a laboratory-scale furnace. Combust. Flame 160 (2013) 933–946.

[6] B. B. Dally, A. N. Karpetis, R. S. Barlow. Structure of turbulent non-premixed jet flames in a diluted hot coflow. Proc. Combust. Inst. 29 (2002) 1147–1154.

[7] B. Zhou, M. Costa, Z. Li, M. Aldén, X. S. Bai. Characterization of the reaction zone structures in a laboratory combustor using optical diagnostics: From flame to flameless combustion. Proc. Combust. Inst. 36 (2017) 4305–4312.

[8] C. Duwig, B. Li, Z. S. Li, M. Aldén. High resolution imaging of flameless

and distributed turbulent combustion. Combust. Flame 159 (2012) 306–316.

[9] J. A. Wagner, M. W. Renfro, B. M. Cetegen. Premixed jet flame behavior in a hot vitiated crossflow of lean combustion products. Combust. Flame 176 (2017) 521–533.

[10] O. Schulz, E. Piccoli, A. Felden, G. Staffelbach, N. Noiray. Autoignition-cascade in the windward mixing layer of a premixed jet in hot vitiated crossflow. Combust. Flame 201 (2019) 215–233.

[11] H. Wang, E. Hawkes, B. Savard, J. Chen. Direct numerical simulation of a high Ka CH4/air stratified premixed jet flame. Combust. Flame 193 (2018) 229–245.

[12] T. M. Wabel, R. S. Barlow, A. M. Steinberg. Reaction zone stratification in piloted highly-turbulent fuel-lean premixed jets. Combust. Flame 208 (2019) 327–329.

[13] M. Ihme, Y. C. See. LES flamelet modeling of a three-stream MILD combustor: Analysis of flame sensitivity to scalar inflow conditions. Proc. Combust. Inst. 33 (2011) 1309–1317.

[14] M. J. Evans, P. R. Medwell, H. Wu, A. Stagni, M. Ihme, I. Chimica, P. Milano. Classification and lift-off height prediction of non-premixed MILD and autoignitive flames. Proc. Combust. Inst. 36 (2017) 4297–4304.

[15] Z. Chen, V. M. Reddy, S. Ruan, N. A. K. Doan, W. L. Roberts,

N. Swaminathan. Simulation of MILD combustion using Perfectly Stirred Reactor model. Proc. Combust. Inst. 36 (2017) 4279–4286.

[16] H. Lu, C. Zou, S. Shao, H. Yao. Large-eddy simulation of MILD combustion using partially stirred reactor approach. Proc. Combust. Inst. 37 (2019) 4507–4518.

[17] J. A. V. Oijen. Direct numerical simulation of autoigniting mixing layers in MILD combustion. Proc. Combust. Inst. 34 (2013) 1163–1171.

[18] Y. Minamoto, T. D. Dunstan, N. Swaminathan, R. S. Cant. DNS of EGR-type turbulent flame in MILD condition. Proc. Combust. Inst. 34 (2013) 3231–3238.

[19] N. Anh, K. Doan, N. Swaminathan, Y. Minamoto. DNS of MILD combustion with mixture fraction variations. Combust. Flame 189 (2018) 173–189.

[20] D. Goodwin, H. Moffat, R. Speth. Cantera: An object-oriented software toolkit for chemical kinetics, thermodynamics, and transport processes (2009).

[21] H. Wang, E. R. Hawkes, J. H. Chen, B. Zhou, Z. Li, M. Aldén. Direct numerical simulations of a high Karlovitz number laboratory premixed jet flame an analysis of flame stretch and flame thickening. J. Fluid Mech. 815 (2017) 511–536.

[22] A. Krisman, E. R. Hawkes, J. H. Chen. The structure and propagation of laminar flames under autoignitive conditions. Combust. Flame 188 (2018) 399–411.

[23] T. Poinsot, S. Lele. Boundary conditions for direct simulations compressible viscous flows. J. Comput. Phys. 101 (1992) 104–129.

[24] J. Chen, A. Choudhary, B. de Supinski, M. DeVries, E. Hawkes, S. Klasky, W. Liao, K. Ma, J. Mellor-Crummey, N. Podhorszki, R. Sankaran, S. Shende, C. Yoo. Terascale direct numerical simulations of turbulent combustion using S3D. Comput. Sci. Discov. 125 (2008) 015001.

[25] Z. Luo, C. S. Yoo, E. S. Richardson, J. H. Chen, C. K. Law, T. Lu. Chemical explosive mode analysis for a turbulent lifted ethylene jet flame in highly-heated coflow. Combust. Flame 159 (2012) 265–274.

[26] T. F. Lu, C. S. Yoo, J. H. Chen, C. K. Law. Three-dimensional direct numerical simulation of a turbulent lifted hydrogen jet flame in heated coflow: a chemical explosive mode analysis. J. Fluid Mech. 652 (2010) 45–64.

[27] C. Xu, J. W. Park, C. S. Yoo, J. H. Chen, T. Lu. Identification of premixed flame propagation modes using chemical explosive mode analysis. Proc. Combust. Inst. 37 (2019) 2407–2415.

[28] R. L. Gordon, A. R. Masri, S. B. Pope, G. M. Goldin. Transport budgets in turbulent lifted flames of methane autoigniting in a vitiated co-flow. Combust. Flame 151 (2007) 495–511.

[29] K. Aditya, A. Gruber, C. Xu, T. Lu, A. Krisman, M. R. Bothien, J. H. Chen. Direct numerical simulation of flame stabilization assisted by

autoignition in a reheat gas turbine combustor. Proc. Combust. Inst. 37 (2019) 2635–2642.

[30] H. Wang, E. R. Hawkes, J. H. Chen. A direct numerical simulation study of flame structure and stabilization of an experimental high Ka CH4/air premixed jet flame. Combust. Flame 180 (2017) 110–123.